

Determination of mass hierarchy with $\nu_\mu \rightarrow \nu_\tau$ appearance and the effect of nonstandard interactions

Ahmed Rashed^{1,2,3,4*}, and Alakabha Datta^{1†}

¹*Department of Physics and Astronomy, University of Mississippi,
Lewis Hall, University, Mississippi, 38677 USA*

²*Department of Physics, Faculty of Science, Ain Shams University, Cairo, 11566, Egypt*

³*Center for Fundamental Physics, Zewail City of Science and Technology, Giza 12588, Egypt*

⁴*The Abdus Salam ICTP, Strada Costiera 11, 34014 Trieste, Italy*

Crucial developments in neutrino physics would be the determination of the mass hierarchy (MH) and measurement of the CP phase in the leptonic sector. The patterns of the transition probabilities $P(\nu_\mu \rightarrow \nu_\tau)$ and $P(\bar{\nu}_\mu \rightarrow \bar{\nu}_\tau)$ are sensitive to these oscillation parameters. An asymmetry parameter can be defined as the difference of these two probabilities normalized to their sum. The profile of the asymmetry parameter gives a clear signal of the mass ordering as it is found to be positive for inverted hierarchy and negative for normal hierarchy. The asymmetry parameter is also sensitive to the CP phase. We consider the effects of non-standard neutrino interactions (NSI) on the determination of the mass hierarchy. Since we assume the largest new physics effects involve the τ sector only, we ignore NSI in production and study the NSI effects in detection as well as along propagation. We find that the NSI effects can significantly modify the prediction of the asymmetry parameter though the MH can still be resolved.

PACS numbers:

After ruling out the zero value of the smallest mixing angle θ_{13} in the lepton sector with C.L. around 5σ [1], the main scope of the future experiments is to answer some open questions such as the absolute mass scale, mass hierarchy, and CP asymmetry in the lepton sector.

Knowledge of the mass hierarchy has an impact on determining the neutrino absolute mass scale, CP asymmetry in the lepton sector, and the nature of the neutrino to be either Dirac or Majorana. Once the ordering of the neutrino mass states is determined, the uncertainty on the measurement of the CP-violating phase, δ_{CP} , is significantly reduced. Measuring the mass ordering can cut down the domain for observation of a signal in the neutrinoless double beta decay experiments. Cosmological measurements are sensitive to the sum of neutrino masses, thus, knowledge of the mass hierarchy could help in determining the absolute neutrino mass scale.

The mass hierarchy (MH) can be determined using different techniques. The transition probability from a neutrino flavor to another, in the presence of matter effect, is sensitive to the mass hierarchy. The shape of the oscillation profile can be used to infer the sign of Δm_{23}^2 thereby indicating whether we have normal hierarchy (NH) or the inverted hierarchy (IH). The standard proposal is to use the appearance channel $\nu_\mu \rightarrow \nu_e$ to measure MH. Determination of mass hierarchy is in the scope of several future experiments such as DUNE [2–5], Hyper-Kamiokande [6, 7], LBNO [8, 9], and INO [10]. A variety of other experiments has some sensitivity to the mass hierarchy such as the reactor neutrino experiments JUNO (formerly known as Daya Bay II) and RENO as well as PINGU [11] at IceCube. The CP asymmetry can be measured in very long base line neutrino experiments such as LBNO (2300 km baseline length) and DUNE (1300 km baseline length) as well as Hyper-K (295 km baseline length). The existence of neutrino masses and mixing require physics beyond the standard model (SM). Hence it is not unexpected that neutrinos could have

* E-mail:amrashed@go.olemiss.edu

† E-mail:datta@phy.olemiss.edu

non-standard interactions (NSI). An important question is how this NSI impact the MH determination or the measurement of the CP violating phase [12]. Even if NSI does not significantly impact the MH determination it will be useful to have alternate channels to confirm the results from the standard channel.

In this work we want to explore MH in the $\nu_\mu \rightarrow \nu_\tau$ channel. Compared to the standard channel, $\nu_\mu \rightarrow \nu_\tau$ has certain advantages. The transition probability for $\nu_\mu \rightarrow \nu_\tau$ is proportional to sine of the atmospheric mixing angle, while $P(\nu_\mu \rightarrow \nu_e)$ is suppressed by small oscillation parameters, such as $\sin^2 \theta_{13}$ and Δm_{12}^2 . We are going to focus, in this paper, on the long baseline DUNE and LBNO experiments. We will also consider NSI effects in our analysis.

There are several reasons to consider NSI involving the (ν_τ, τ) sector. First, the third generation may be more sensitive to new physics effects because of their larger masses. As an example, in certain versions of the two Higgs doublet models (2HDM) the couplings of the new Higgs bosons are proportional to the masses and so new physics effects are more pronounced for the third generation. Second, the constraints on new physics (NP) involving the third generation leptons are somewhat weaker allowing for larger new physics effects.

A key property of the SM gauge interactions is that they are lepton flavor universal. Evidence for violation of this property would be a clear sign of new physics (NP) beyond the SM. Interestingly, there have been some reports of non universality in the lepton sector from experiments. In the charged current sector the decays $\bar{B} \rightarrow D^{(*)+} \ell^- \bar{\nu}_\ell$, have been measured by the BaBar [13], Belle [14] and LHCb [15] Collaborations. It is found that the values of the ratios $\mathcal{B}(\bar{B} \rightarrow D^{(*)+} \tau^- \bar{\nu}_\tau) / \mathcal{B}(\bar{B} \rightarrow D^{(*)+} \ell^- \bar{\nu}_\ell)$ ($\ell = e, \mu$) deviate from the SM predictions [16] and this could be indication of lepton non universal new physics[17]. Specifically, [18]

$$\begin{aligned} R_D &\equiv \frac{\mathcal{B}(\bar{B} \rightarrow D^+ \tau^- \bar{\nu}_\tau)_{\text{expt}} / \mathcal{B}(\bar{B} \rightarrow D^+ \tau^- \bar{\nu}_\tau)_{\text{SM}}}{\mathcal{B}(\bar{B} \rightarrow D^+ \ell^- \bar{\nu}_\ell)_{\text{expt}} / \mathcal{B}(\bar{B} \rightarrow D^+ \ell^- \bar{\nu}_\ell)_{\text{SM}}} = 1.37 \pm 0.18 , \\ R_{D^*} &\equiv \frac{\mathcal{B}(\bar{B} \rightarrow D^{*+} \tau^- \bar{\nu}_\tau)_{\text{expt}} / \mathcal{B}(\bar{B} \rightarrow D^{*+} \tau^- \bar{\nu}_\tau)_{\text{SM}}}{\mathcal{B}(\bar{B} \rightarrow D^{*+} \ell^- \bar{\nu}_\ell)_{\text{expt}} / \mathcal{B}(\bar{B} \rightarrow D^{*+} \ell^- \bar{\nu}_\ell)_{\text{SM}}} = 1.28 \pm 0.08 . \end{aligned} \quad (1)$$

The measured values of R_D and R_{D^*} represent deviations from the SM of 2.0σ and 3.8σ , respectively. There also appears to be violation of lepton universality in $W\tau\nu_\tau$ coupling though it is difficult to explain [19].

There has been another recent hint of lepton non-universality in the neutral current sector. The LHCb Collaboration measured the ratio of decay rates for $B^+ \rightarrow K^+ \ell^+ \ell^-$ ($\ell = e, \mu$) in the dilepton invariant mass-squared range $1 \text{ GeV}^2 \leq q^2 \leq 6 \text{ GeV}^2$ [20], and found

$$\begin{aligned} R_K &\equiv \frac{\mathcal{B}(B^+ \rightarrow K^+ \mu^+ \mu^-)}{\mathcal{B}(B^+ \rightarrow K^+ e^+ e^-)} \\ &= 0.745_{-0.074}^{+0.090} (\text{stat}) \pm 0.036 (\text{syst}) . \end{aligned} \quad (2)$$

This differs from the SM prediction of $R_K = 1 \pm O(10^{-4})$ [21] by 2.6σ .

These measurements might be hinting towards lepton non universal new physics with the largest effects involving the third generation leptons [22]. The new physics could arise in the third generation and feed down to other generation through mixing effects and so in this picture we expect the largest NSI to involve the third generation neutrino. In our analysis, therefore, we will assume NSI only involving the third generation leptons.

The tau-neutrino appearance channel is relevant to the Long Baseline Neutrino Oscillation Experiment (LBNO) which has an access to both transitions $\nu_\mu \rightarrow \nu_\tau$ and $\bar{\nu}_\mu \rightarrow \bar{\nu}_\tau$. The experiment consists of a near detector at CERN in addition to a far detector situated at Pyhäsalmi in Finland 2300 km away from CERN, where the source of neutrino beam is located. The muon- neutrino and anti-neutrino fluxes fall in the energy range of 0 – 10 GeV where it peaks at 5 GeV [8]. This means that the quasi-elastic neutrino interaction is dominant in the energy range of the experiment.

An upcoming experiment is the Deep Underground Neutrino Experiment (DUNE) experiment which has a program to make precise measurements of the mixing between the neutrinos, CP violation, and the ordering of neutrino masses. The two main oscillation channels are $\nu_\mu \rightarrow \nu_e$ and

$\bar{\nu}_\mu \rightarrow \bar{\nu}_e$, but access to $\nu_\mu \rightarrow \nu_\tau$ and $\bar{\nu}_\mu \rightarrow \bar{\nu}_\tau$ modes is possible. The baseline of DUNE is 1300 km and the flux of the neutrino beam ranges from 0-10 GeV [5].

In table 3 in Ref. [8], one can find a comparison between LBNO and DUNE. In the case of LBNO, the expected number of events in the channel $\nu_\mu \rightarrow \nu_\tau$ that comes from charged current interactions is 215/239 for NH/IH, while the number for $\bar{\nu}_\mu \rightarrow \bar{\nu}_\tau$ is anticipated to be 98/99 for NH/IH in 2.5 years of data-taking. The DUNE will observe less number of events in these channels.

The pattern of the transition probability of $\nu_\mu \rightarrow \nu_\tau$ depends on the sign of Δm_{23}^2 and the CP violating phase δ , so one can extract information on MH and the CP phase from this probability. An asymmetry parameter A can be defined as the difference of the two transition probabilities $P(\nu_\mu \rightarrow \nu_\tau)$ and $P(\bar{\nu}_\mu \rightarrow \bar{\nu}_\tau)$ normalized to their sum. The MH can be sensitive to the sign of the asymmetry and the size of the asymmetry can carry some sensitivity to the CP violating phase δ .

We also consider the NSI effects on the determination of MH. The NSI effects can arise at the source, along propagation and at detection. Assuming significant NSI only involving the third generation we will ignore NSI at the source. In any new physics model NSI in propagation and detection are connected. However, we will not use specific models and instead will adopt an effective Lagrangian description of the new physics effects. The NSI effects are parameterized by some co-efficients that depend on the parameters in the effective Lagrangian and we will use experiments to constrain the size of these effects. Along propagation we will consider the effects of the NSI parameters ($\varepsilon_{\mu\tau}, \varepsilon_{\tau\tau}$) to the transition probability pattern ([23–25]). For simplicity we will assume the NSI parameters to be real. Discussion on the impact of NSI parameters (moduli and phases) for CP violation measurement using $P(\nu_\mu \rightarrow \nu_e)$ for the DUNE experiment can be found in Ref. [29].

In previous work [26–28] we introduced NSI at detection and considered various phenomenology connected to neutrino physics. For NSI at detection we use the following picture. The measurement of the transition probability $P(\nu_\mu \rightarrow \nu_\tau)$ can be expressed as [31]:

$$N(\nu_\tau) = P(\nu_\mu \rightarrow \nu_\tau) \times \Phi(\nu_\mu) \times \sigma_{\text{SM}}(\nu_\tau), \quad (3)$$

where $N(\nu_\tau)$ is the number of observed events, $\Phi(\nu_\mu)$ is the flux of muon neutrinos at the detector, $\sigma_{\text{SM}}(\nu_\tau)$ is the total cross section of tau neutrino interactions with nucleons in the SM at the detector, and $P(\nu_\mu \rightarrow \nu_\tau)$ is the probability for the flavor transition $\nu_\mu \rightarrow \nu_\tau$ in the presence of matter effect. In the presence of NSI at the detector, Eq. 3 is modified as

$$N(\nu_\tau) = P_{\text{tot}}(\nu_\mu \rightarrow \nu_\tau) \times \Phi(\nu_\mu) \times \sigma_{\text{tot}}(\nu_\tau), \quad (4)$$

with $\sigma_{\text{tot}}(\nu_\tau) = \sigma_{\text{SM}}(\nu_\tau) + \sigma_{\text{NP}}(\nu_\tau)$, where $\sigma_{\text{NP}}(\nu_\tau)$ refers to the additional terms to the SM contribution towards the total cross section. Hence, $\sigma_{\text{NP}}(\nu_\tau)$ includes contributions from both the SM and NP interference amplitudes, and the pure NP amplitude. From Eqs. (3, 4)

$$P_{\text{tot}}(\nu_\mu \rightarrow \nu_\tau) = P(\nu_\mu \rightarrow \nu_\tau) \frac{\sigma_{\text{SM}}(\nu_\tau)}{\sigma_{\text{tot}}(\nu_\tau)}. \quad (5)$$

Moving on to the transition probabilities, we define the asymmetry parameter as the difference between the neutrino and anti-neutrino transition probabilities normalized to their sum

$$A = \frac{P_{\text{tot}}(\nu_\mu \rightarrow \nu_\tau) - P_{\text{tot}}(\bar{\nu}_\mu \rightarrow \bar{\nu}_\tau)}{P_{\text{tot}}(\nu_\mu \rightarrow \nu_\tau) + P_{\text{tot}}(\bar{\nu}_\mu \rightarrow \bar{\nu}_\tau)}. \quad (6)$$

In the limit where matter effects are neglected A is just a measure of CP violation.

The transition probability of the appearance channel $\nu_\mu - \nu_\tau$ in the presence of matter effect and NSI along propagation is given as [32–35]

$$\begin{aligned} P(\nu_\alpha \rightarrow \nu_\beta; \varepsilon_{e\mu}, \varepsilon_{e\tau}, \varepsilon_{\mu\mu}, \varepsilon_{\mu\tau}, \varepsilon_{\tau\tau}) &= P(\nu_\alpha \rightarrow \nu_\beta; 2 \text{ flavor in vacuum}) \\ &+ P(\nu_\alpha \rightarrow \nu_\beta; \varepsilon_{e\mu}, \varepsilon_{e\tau}) \\ &+ P(\nu_\alpha \rightarrow \nu_\beta; \varepsilon_{\mu\mu}, \varepsilon_{\mu\tau}, \varepsilon_{\tau\tau}), \end{aligned} \quad (7)$$

where α and β denote one of μ and τ , and ε 's are the NSI parameters. The first term in Eq. 7 has a form that it appears in the two flavor oscillation in vacuum:

$$P(\nu_\mu \rightarrow \nu_\tau; 2 \text{ flavor in vacuum}) = 4c_{23}^2 s_{23}^2 \sin^2 \frac{\Delta m_{31}^2 L}{4E}, \quad (8)$$

where $s_{ij} \equiv \sin \theta_{ij}$ and $c_{ij} \equiv \cos \theta_{ij}$. The second and third terms in the oscillation probability in the $\nu_\mu \rightarrow \nu_\tau$ channel are given by

$$\begin{aligned} & P(\nu_\mu \rightarrow \nu_\tau; \varepsilon_{e\mu}, \varepsilon_{e\tau}) \\ &= 4c_{23}^2 s_{23}^2 |\Xi|^2 \left(\frac{aL}{4E} \right) \sin \frac{\Delta m_{31}^2 L}{2E} - 8c_{23}^2 s_{23}^2 |\Xi|^2 \sin \frac{aL}{4E} \sin \frac{\Delta m_{31}^2 L}{4E} \cos \frac{\Delta m_{31}^2 - a}{4E} L \\ &+ 4c_{23}^2 s_{23}^2 |\Theta_\pm|^2 \left(\frac{a}{\Delta m_{31}^2 - a} \right) \left(\frac{aL}{4E} \right) \sin \frac{\Delta m_{31}^2 L}{2E} \\ &- 8c_{23}^2 s_{23}^2 |\Theta_\pm|^2 \left(\frac{a}{\Delta m_{31}^2 - a} \right)^2 \cos \frac{aL}{4E} \sin \frac{\Delta m_{31}^2 L}{4E} \sin \frac{\Delta m_{31}^2 - a}{4E} L \\ &+ 8c_{23} s_{23} (c_{23}^2 - s_{23}^2) |\Xi| |\Theta_\pm| \cos(\xi - \theta_\pm) \left(\frac{a}{\Delta m_{31}^2 - a} \right) \left(\frac{a}{\Delta m_{31}^2} \right) \sin^2 \frac{\Delta m_{31}^2 L}{4E} \\ &+ 8c_{23} s_{23} |\Xi| |\Theta_\pm| \left(\frac{a}{\Delta m_{31}^2 - a} \right) \sin \frac{aL}{4E} \sin \frac{\Delta m_{31}^2 L}{4E} \\ &\quad \times \left[s_{23}^2 \cos \left(\xi - \theta_\pm - \frac{\Delta m_{31}^2 - a}{4E} L \right) - c_{23}^2 \cos \left(\xi - \theta_\pm + \frac{\Delta m_{31}^2 - a}{4E} L \right) \right], \quad (9) \end{aligned}$$

and

$$\begin{aligned} & P(\nu_\mu \rightarrow \nu_\tau; \varepsilon_{\mu\mu}, \varepsilon_{\mu\tau}, \varepsilon_{\tau\tau}) \\ &= -2c_{23}^2 s_{23}^2 \left(s_{13}^2 \frac{\Delta m_{31}^2}{a} - \mathcal{S}_1 \right) \left(\frac{aL}{2E} \right) \sin \frac{\Delta m_{31}^2 L}{2E} + c_{23}^2 s_{23}^2 \mathcal{S}_1^2 \left(\frac{aL}{2E} \right)^2 \cos \frac{\Delta m_{31}^2 L}{2E} \\ &- 8c_{23} s_{23} (c_{23}^2 - s_{23}^2) \left[c_{12} s_{12} s_{13} \cos \delta \left(\frac{\Delta m_{21}^2}{a} \right) - |\mathcal{E}| \cos \phi \right] \left(\frac{a}{\Delta m_{31}^2} \right) \sin^2 \frac{\Delta m_{31}^2 L}{4E} \\ &+ 4c_{23} s_{23} (c_{23}^2 - s_{23}^2) \mathcal{S}_1 |\mathcal{E}| \cos \phi \left(\frac{a}{\Delta m_{31}^2} \right) \left[\left(\frac{aL}{2E} \right) \sin \frac{\Delta m_{31}^2 L}{2E} - 2 \left(\frac{a}{\Delta m_{31}^2} \right) \sin^2 \frac{\Delta m_{31}^2 L}{4E} \right] \\ &+ 4c_{23}^2 s_{23}^2 |\mathcal{E}|^2 \left(\frac{a}{\Delta m_{31}^2} \frac{aL}{2E} \right) \sin \frac{\Delta m_{31}^2 L}{2E} \\ &+ 4|\mathcal{E}|^2 \left[(c_{23}^2 - s_{23}^2)^2 - 4c_{23}^2 s_{23}^2 \cos^2 \phi \right] \left(\frac{a}{\Delta m_{31}^2} \right)^2 \sin^2 \frac{\Delta m_{31}^2 L}{4E}. \quad (10) \end{aligned}$$

The subscript \pm in these equations denote the normal and the inverted mass hierarchies, which corresponds to the positive and negative values of Δm_{32}^2 . The simplified notations which involve ε 's in the $\nu_\mu - \nu_\tau$ sector are as follows:

$$\begin{aligned} \Theta_\pm &\equiv s_{13} \frac{\Delta m_{31}^2}{a} + (s_{23} \varepsilon_{e\mu} + c_{23} \varepsilon_{e\tau}) e^{i\delta} \equiv |\Theta_\pm| e^{i\theta_\pm}, \\ \Xi &\equiv \left(c_{12} s_{12} \frac{\Delta m_{21}^2}{a} + c_{23} \varepsilon_{e\mu} - s_{23} \varepsilon_{e\tau} \right) e^{i\delta} \equiv |\Xi| e^{i\xi}, \\ \mathcal{E} &\equiv c_{23} s_{23} (\varepsilon_{\mu\mu} - \varepsilon_{\tau\tau}) + c_{23}^2 \varepsilon_{\mu\tau} - s_{23}^2 \varepsilon_{\mu\tau}^* \equiv |\mathcal{E}| e^{i\phi}, \\ \mathcal{S}_1 &\equiv (c_{23}^2 - s_{23}^2) (\varepsilon_{\tau\tau} - \varepsilon_{\mu\mu}) + 2c_{23} s_{23} (\varepsilon_{\mu\tau} + \varepsilon_{\mu\tau}^*) - c_{12}^2 \frac{\Delta m_{21}^2}{a}. \quad (11) \end{aligned}$$

We also note that Θ_{\pm} , Ξ , and \mathcal{E} are complex numbers while \mathcal{S}_1 is real. The matter potential is given by

$$\begin{aligned} a &= 2\sqrt{2}G_F N_e E \\ &= 7.6324 \times 10^{-5} \text{eV}^2 \frac{\rho}{\text{gcm}^{-3}} \frac{E}{\text{GeV}}. \end{aligned} \quad (12)$$

Using the Preliminary Reference Earth Model (PREM) [36], the line-averaged constant matter density is $\rho = 3.54 \text{ g/cm}^3$ for the LBNO baseline of $L = 2300 \text{ km}$ which corresponds to the distance between CERN and Pyhäsalmi [9, 37, 38]. For the DUNE experiment, we use the standard value of the matter density $\rho = 2.8 \text{ g/cm}^3$. In matter, the probability for T conjugate channels is obtained by the replacement $\delta \rightarrow -\delta$ and those for CP conjugate channels are obtained by $\delta \rightarrow -\delta$ and $a \rightarrow -a$.

In Fig. 1 we show $P(\nu_{\mu} \rightarrow \nu_{\tau})$ and its CP conjugate channel in the LBNO energy range. Here, we consider no NSI along propagation $(\varepsilon_{\mu\tau}, \varepsilon_{\tau\tau}) = (0, 0)$ (top panel) and with experimental upper bound of $(\varepsilon_{\mu\tau}, \varepsilon_{\tau\tau}) = (0.07, 0.147)$ (bottom panel) ([23–25]). Other NSI parameters are taken to be zero. In Fig. 2, we show the asymmetry parameter A which is positive for IH and decreases with energy, while it is negative for NH and increases with energy for $(\varepsilon_{\mu\tau}, \varepsilon_{\tau\tau}) = (0, 0)$. In the presence of NSI $(\varepsilon_{\mu\tau}, \varepsilon_{\tau\tau}) = (0.07, 0.147)$, A changes sign for both the hierarchies. The asymmetry profile for the two hierarchies has a crossing point where the MH cannot be resolved. The shape of the A parameter in this case can therefore resolve the MH (except at the crossing point) and provides clear evidence of NSI. One can notice that that A parameter is sensitive to the CP phase. The same plots for the energy range and baseline relevant to DUNE experiment are shown in Figs. (3, 4). Compared to LBNO results, one can find that the asymmetry parameter has smaller values with considering no NSI along propagation and so it will be difficult to resolve the MH. In this case, A , does not flip sign, in the desired energy range, when NSI along propagation is included. However, at larger energies in the presence of NSI, A is substantially different for the two hierarchies so that the MH can be resolved.

Now, we study the effects of new physics contributions to the tau-neutrino interactions at the detector on the pattern of the asymmetry parameter A in the energy range relevant to LBNO and DUNE. Adopting an effective Hamiltonian approach we include generic vector axial-vector, scalar, and tensor interactions. In the LBNO and DUNE energy range, the quasielastic tau neutrino scattering is dominant.

In the presence of NP, the effective Hamiltonian for the scattering process $\nu_{\ell} + n \rightarrow \ell^{-} + p$ can be written in the form [39],

$$\begin{aligned} \mathcal{H}_{\text{eff}} &= \frac{4G_F V_{ud}}{\sqrt{2}} \left[(1 + V_L) [\bar{u}\gamma^{\mu} P_L d] [\bar{l}\gamma_{\mu} P_L \nu_l] + V_R [\bar{u}\gamma^{\mu} P_R d] [\bar{l}\gamma_{\mu} P_L \nu_l] \right. \\ &\quad \left. + S_L [\bar{u} P_L d] [\bar{l} P_L \nu_l] + S_R [\bar{u} P_R d] [\bar{l} P_L \nu_l] + T_L [\bar{u}\sigma^{\mu\nu} P_L d] [\bar{l}\sigma_{\mu\nu} P_L \nu_l] \right], \end{aligned} \quad (13)$$

where $G_F = 1.1663787(6) \times 10^{-5} \text{ GeV}^{-2}$ is the Fermi coupling constant, V_{ud} is the Cabibbo-Kobayashi-Maskawa (CKM) matrix element, $P_{L,R} = (1 \mp \gamma_5)/2$ are the projectors of negative/positive chiralities. We assume the neutrino to be always left chiral. The Hamiltonian can be written as,

$$\begin{aligned} \mathcal{H}_{\text{eff}} &= \frac{G_F V_{ud}}{\sqrt{2}} \left\{ [\bar{u}\gamma^{\mu}(1 - \gamma_5)d] [\bar{l}\gamma_{\mu}(1 - \gamma_5)\nu_l] + [\bar{u}(A_S + B_S\gamma_5)d] [\bar{l}(1 - \gamma_5)\nu_l] \right. \\ &\quad \left. + [\bar{u}\gamma^{\mu}(A_V + B_V\gamma_5)d] [\bar{l}\gamma_{\mu}(1 - \gamma_5)\nu_l] + T_L [\bar{u}\sigma^{\mu\nu}(1 - \gamma_5)d] [\bar{l}\sigma_{\mu\nu}(1 - \gamma_5)\nu_l] \right\}, \end{aligned} \quad (14)$$

where $A_S = S_R + S_L$, $B_S = S_R - S_L$, $A_V = V_R + V_L$ and $B_V = V_R - V_L$ with S_L and S_R are the left and right handed scalar couplings, V_L and V_R are the left and right handed vector couplings and T_L is the tensor coupling. The operators that describe the process $\bar{\nu}_{\ell} + p \rightarrow \ell^{+} + n$ can be obtained from the hermitian conjugate of the above Hamiltonian. The co-efficients in the effective Hamiltonian are fixed by low energy observables such as τ decays [26–28].

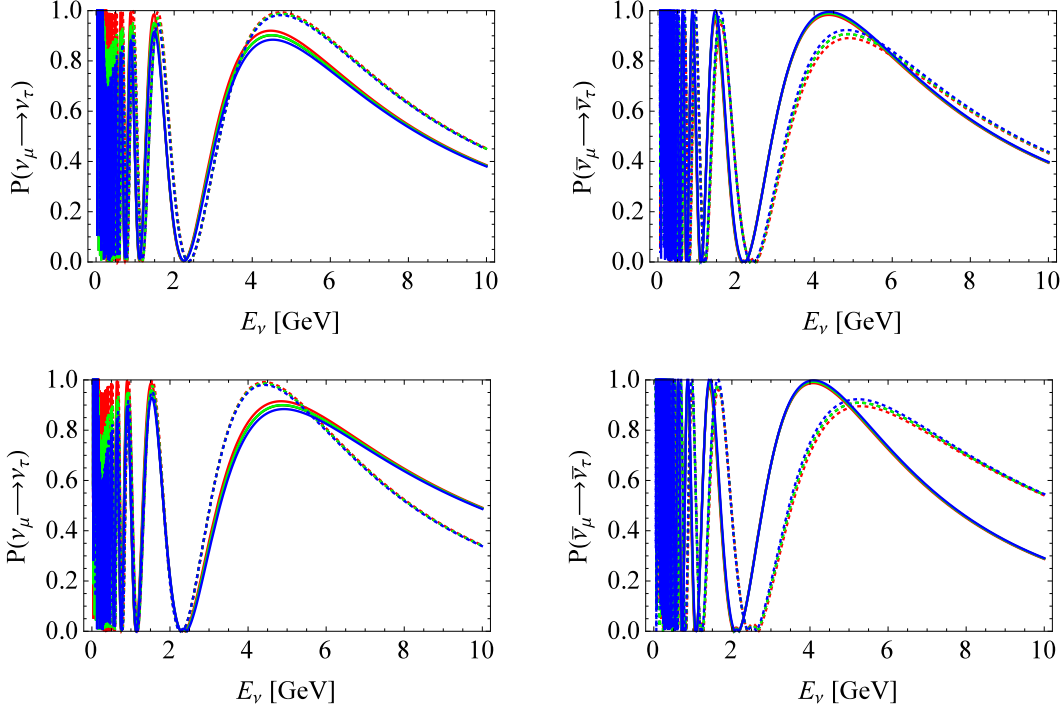


FIG. 1: The transition probability of the $\nu_\mu \rightarrow \nu_\tau$ (left) channel and its CP conjugate channel $\bar{\nu}_\mu \rightarrow \bar{\nu}_\tau$ (right) in the presence of matter effect for the LBNO energy range and baseline. The solid/dotted lines correspond to NH/IH. The green, red, and blue lines correspond to $\delta = (0, \pi/2, -\pi/2)$, respectively. NSI parameters are taken to be $(\varepsilon_{\mu\tau}, \varepsilon_{\tau\tau}) = (0, 0)$ (top) and $(\varepsilon_{\mu\tau}, \varepsilon_{\tau\tau}) = (0.07, 0.147)$ (bottom).

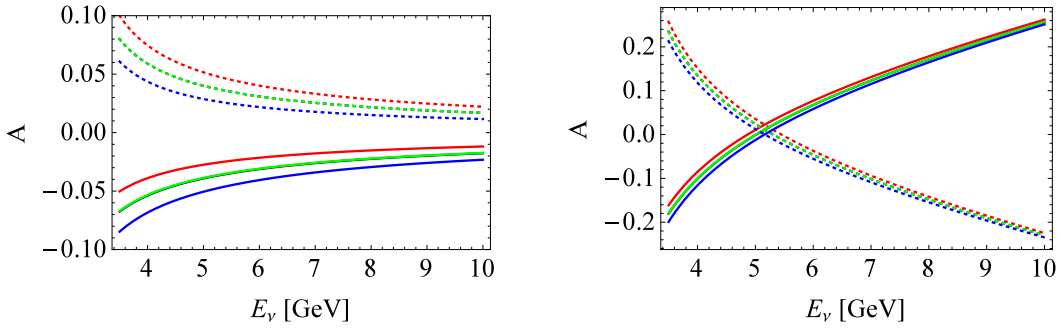


FIG. 2: The asymmetry parameter A for the LBNO energy range and baseline length. The solid/dotted lines correspond to NH/IH. The green, red, and blue lines correspond to $\delta = (0, \pi/2, -\pi/2)$, respectively. NSI parameters are taken to be $(\varepsilon_{\mu\tau}, \varepsilon_{\tau\tau}) = (0, 0)$ (left) and $(\varepsilon_{\mu\tau}, \varepsilon_{\tau\tau}) = (0.07, 0.147)$ (right).

In $\nu_\tau + n \rightarrow \tau^- + p$ the hadronic effects are described in terms of form factors. We define the charged hadronic current for the process $\nu_\tau + n \rightarrow \tau^- + p$ in the SM as

$$\begin{aligned} \langle p(p') | J_\mu^+ | n(p) \rangle &= \langle p(p') | (V_\mu - A_\mu) | n(p) \rangle \\ &= V_{ud} \bar{p}(p') \Gamma_\mu n(p), \end{aligned} \quad (15)$$

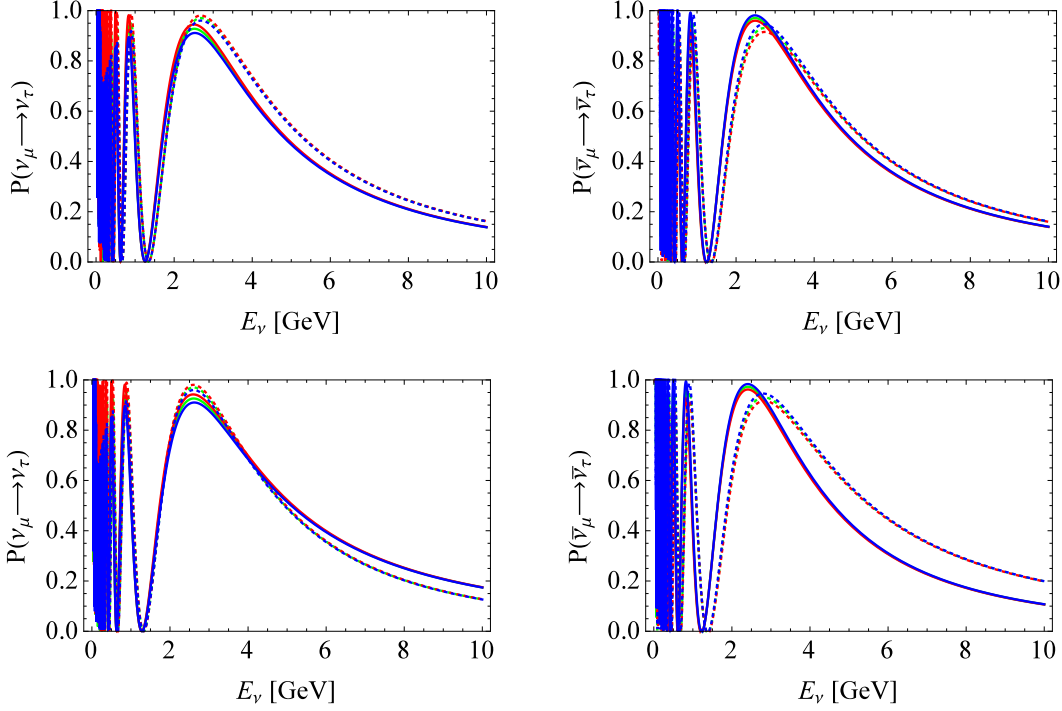


FIG. 3: The transition probability of the $\nu_\mu \rightarrow \nu_\tau$ (left) channel and its CP conjugate channel $\bar{\nu}_\mu \rightarrow \bar{\nu}_\tau$ (right) in the presence of matter effect for the DUNE energy range and baseline. The solid/dotted lines correspond to NH/IH. The green, red, and blue lines correspond to $\delta = (0, \pi/2, -\pi/2)$, respectively. NSI parameters are taken to be $(\varepsilon_{\mu\tau}, \varepsilon_{\tau\tau}) = (0, 0)$ (top) and $(\varepsilon_{\mu\tau}, \varepsilon_{\tau\tau}) = (0.07, 0.147)$ (bottom).

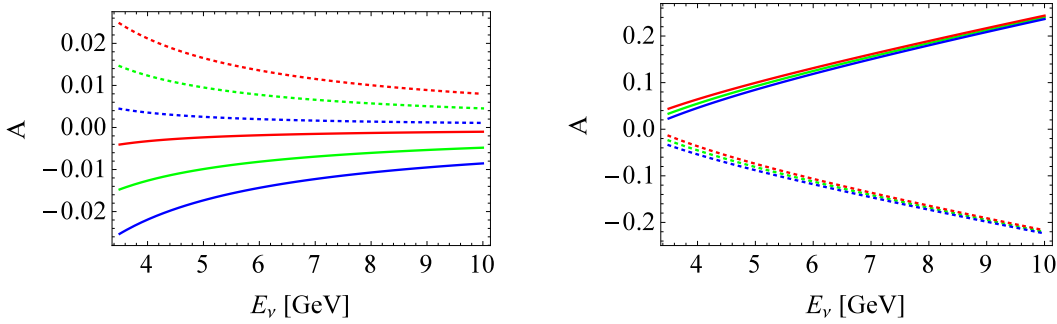


FIG. 4: The asymmetry parameter A for the DUNE energy range and baseline length. The solid/dotted lines correspond to NH/IH. The green, red, and blue lines correspond to $\delta = (0, \pi/2, -\pi/2)$, respectively. NSI parameters are taken to be $(\varepsilon_{\mu\tau}, \varepsilon_{\tau\tau}) = (0, 0)$ (left) and $(\varepsilon_{\mu\tau}, \varepsilon_{\tau\tau}) = (0.07, 0.147)$ (right).

with

$$\Gamma_\mu = \left[F_1^V(t)\gamma_\mu + F_2^V(t)i\frac{\sigma_{\mu\nu}q^\nu}{2M} + F_A(t)\gamma_\mu\gamma_5 + F_P(t)\gamma_5\frac{q_\mu}{M} \right]. \quad (16)$$

Here F 's are the hadronic form factors which are functions of the squared momentum transfer t .

The expressions for the vector and axial-vector hadronic currents in Eq. 15 are

$$\begin{aligned}\langle p(p')|V_\mu|n(p)\rangle &= V_{ud}\bar{p}(p')\left[\gamma_\mu F_1^V(t) + \frac{i}{2M}\sigma_{\mu\nu}q^\nu F_2^V(t)\right]n(p), \\ -\langle p(p')|A_\mu|n(p)\rangle &= V_{ud}\bar{p}(p')\left[\gamma_\mu F_A(t) + \frac{q_\mu}{M}F_P(t)\right]\gamma_5 n(p).\end{aligned}\quad (17)$$

Similarly, in the presence of (A_V, B_V) ,

$$\langle p(p')|J_\mu^+|n(p)\rangle = \langle p(p')|(A_V V_\mu + B_V A_\mu)|n(p)\rangle, \quad (18)$$

with

$$\begin{aligned}\langle p(p')|A_V V_\mu|n(p)\rangle &= V_{ud}A_V\bar{p}(p')\left[\gamma_\mu F_1^V(t) + \frac{i}{2M}\sigma_{\mu\nu}q^\nu F_2^V(t)\right]n(p), \\ \langle p(p')|B_V A_\mu|n(p)\rangle &= -V_{ud}B_V\bar{p}(p')\left[\gamma_\mu F_A(t) + \frac{q_\mu}{M}F_P(t)\right]\gamma_5 n(p).\end{aligned}\quad (19)$$

The scalar current for the process $\nu_\tau + n \rightarrow \tau^- + p$ can be parametrized as follows

$$\begin{aligned}\langle p(p')|J^+|n(p)\rangle &= \langle p(p')|\bar{u}(A_S + B_S\gamma_5)d|n(p)\rangle \\ &= V_{ud}\bar{p}(p')(A_S G_S + B_S G_P\gamma_5)n(p).\end{aligned}\quad (20)$$

Using the equation of motion,

$$\begin{aligned}G_S(t) &= r_N F_1^V(t), \quad \text{with } r_N = \frac{M_n - M_p}{m_d - m_u} \sim \mathcal{O}(1), \\ G_P(t) &= -\left(F_A(t)\left(\frac{M_n - M_p}{m_d - m_u}\right) + F_P(t)\frac{m_d + m_u}{M}\right),\end{aligned}\quad (21)$$

with $m_u = 2.3$ MeV and $m_d = 4.8$ MeV [30].

In the presence of tensor state, the tensor current can be parametrized as follows

$$\begin{aligned}\langle p(p')|J^{\mu\nu}|n(p)\rangle &= \langle p(p')|\bar{u}\sigma^{\mu\nu}(1 - \gamma_5)d|n(p)\rangle \\ &= iV_{ud}K_{S,P}\bar{p}(p')(\Gamma^\mu\tilde{\Gamma}^\nu - \tilde{\Gamma}^\mu\Gamma^\nu)n(p) \\ &= \frac{i}{2M}V_{ud}\bar{p}(p')(K_S\Pi_1^{\mu\nu} - K_P\Pi_2^{\mu\nu}\gamma_5)n(p),\end{aligned}\quad (22)$$

with $\tilde{\Gamma}$ defined as

$$\begin{aligned}\tilde{\Gamma}^\mu(p, p') &= \gamma_0\Gamma^{\mu\dagger}(p', p)\gamma_0, \\ &= \left[F_1^V(t)\gamma_\mu - F_2^V(t)i\frac{\sigma_{\mu\nu}q^\nu}{2M} + F_A(t)\gamma_\mu\gamma_5 - F_P(t)\gamma_5\frac{q_\mu}{M}\right],\end{aligned}\quad (23)$$

and

$$\begin{aligned}K_S &= -\frac{M(M_p^2 - M_n^2) - (m_u^2 - m_d^2)}{4t(M_p - M_n)}\frac{G_S}{F_A F_P}, \\ K_P &= -\frac{M(M_p^2 - M_n^2) - (m_u^2 - m_d^2)}{4t(M_p + M_n)}\frac{G_P}{F_1 F_P},\end{aligned}\quad (24)$$

with

$$\begin{aligned}\Pi_1^{\mu\nu} &= F_1 F_2(\gamma^\mu\gamma^\nu\rlap{\not{q}} - 2\gamma^\mu\rlap{\not{q}}\gamma^\nu + \rlap{\not{q}}\gamma^\mu\gamma^\nu) - 4F_A F_P(\gamma^\nu q^\mu + \gamma^\mu q^\nu), \\ \Pi_2^{\mu\nu} &= F_A F_2(\gamma^\mu\gamma^\nu\rlap{\not{q}} - 2\gamma^\mu\rlap{\not{q}}\gamma^\nu + \rlap{\not{q}}\gamma^\mu\gamma^\nu) - 4F_1 F_P(\gamma^\nu q^\mu + \gamma^\mu q^\nu).\end{aligned}\quad (25)$$

The total differential cross section is

$$\frac{d\sigma_{tot}(\nu)}{dt} = \frac{G_F^2 \cos^2 \theta_c}{32\pi E_\nu^2 M^2} [A_{tot} + B_{tot} (s - u) + C_{tot} (s - u)^2], \quad (26)$$

with

$$\begin{aligned} A_{tot} &= 16M^4(x_t - x_l) [A_{V\pm A} + A_{Sr} + A_T + A_{V\pm A-Sr} + A_{V\pm A-T}], \\ B_{tot} &= 8M^2 [B_{V\pm A} + B_{V\pm A-Sr} + B_{V\pm A-T} + B_{Sr-T} + B_T], \\ C_{tot} &= C_{V\pm A} + C_T, \end{aligned} \quad (27)$$

where

$$\begin{aligned} A_{V\pm A} &= (1 + A_V)^2 [F_1^2(1 + x_l + x_t) + F_2^2(x_l + x_t^2 + x_t) + 2F_1F_2(x_l + 2x_t)] \\ &\quad + (1 - B_V)^2 [F_A^2(-1 + x_l + x_t) + 4F_P^2x_lx_t + 4F_AF_Px_l], \\ A_{Sr} &= A_S^2G_S^2(x_t - 1) + B_S^2G_P^2x_t, \\ A_T &= 64T_L^2F_2^2(F_1^2K_S^2(x_t - 1)(x_l + x_t) + F_A^2K_P^2(x_lx_t + x_l + x_t^2)), \\ A_{V\pm A-Sr} &= -2(1 - B_V)B_SG_P\sqrt{x_l}(F_A + 2F_Px_t) \left(1 - 4x_t\frac{M^2}{M_W^2}\right), \\ A_{V\pm A-T} &= -32(1 - B_V)T_LK_SF_1F_2F_A\sqrt{x_l}(x_t - 1) + 16(1 + A_V)F_2F_AK_P T_L\sqrt{x_l}(2F_1x_t + F_1 + 3F_2x_t), \end{aligned} \quad (28)$$

$$\begin{aligned} B_{V\pm A} &= 2(1 + A_V)(1 - B_V)x_tF_AF_A(F_1 + F_2), \\ B_{V\pm A-Sr} &= (1 + A_V)A_SG_S\sqrt{x_l}(F_1 + F_2x_t), \\ B_{V\pm A-T} &= -16(1 + A_V)T_LK_Sx_t\sqrt{x_l}F_1F_2(F_1 + F_2) + 16(1 - B_V)T_LK_Px_t\sqrt{x_l}F_2F_A^2, \\ B_{Sr-T} &= 8A_SG_SF_2x_tF_AK_P T_L, \\ B_T &= -128T_L^2x_tx_lF_1F_2^2F_AK_SK_P, \end{aligned} \quad (29)$$

$$\begin{aligned} C_{V\pm A} &= (1 + A_V)^2(F_1^2 - x_tF_2^2) + (1 - B_V)^2F_A^2, \\ C_T &= -64T_L^2F_2^2x_t(F_A^2K_P^2 + F_1^2K_S^2). \end{aligned} \quad (30)$$

Here, $V\pm A$ stands for the SM and (A_V, B_V) contributions, Sr for scalar, and T for tensor. $x_t = t/4M^2$ and $x_l = m_\tau^2/4M^2$ where M and m_τ are the nucleon and tau masses. s, u, t are the Mandelstam variables

For the sake of simplicity we will consider two new physics scenarios. In one we have $S + T$ interactions and in the other $V \pm A$ interactions. Leptoquark models for instance produce both S and T interactions while models with extra gauge bosons have V and A interactions.

The quasielastic scattering of an antineutrino on a free nucleon is given by

$$\bar{\nu}_\tau(k) + p(p) \rightarrow \tau^+(k') + n(p'). \quad (31)$$

The charged hadronic current in SM becomes [40, 41]

$$\begin{aligned} \langle n(p') | J_\mu^- | p(p) \rangle &= \langle p(p) | J_\mu^+ | n(p') \rangle^\dagger \\ &= V_{ud} \bar{n}(p') \tilde{\Gamma}_\mu p(p), \end{aligned} \quad (32)$$

where $\tilde{\Gamma}_\mu$ is defined in Eq. 23.

By comparing the processes $\nu_\tau + n \rightarrow \tau^- + p$ and $\bar{\nu}_\tau + p \rightarrow \tau^+ + n$, the expression of the differential cross section for anti-neutrino scattering can be obtained from the one for neutrino interaction by

making the following changes: $F_P \rightarrow -F_P$, $F_2^V \rightarrow -F_2^V$, $(s - u) \rightarrow -(s - u)$, $M_p \leftrightarrow M_n$, and $m_u \leftrightarrow m_d$.

The scalar and tensor currents for the process $\bar{\nu}_\tau + p \rightarrow \tau^+ + n$ are parametrized as

$$\begin{aligned} \langle n(p') | J^- | p(p) \rangle &= \langle n(p') | \bar{d}(A_S - B_S \gamma_5) u | p(p) \rangle \\ &= V_{ud} \bar{n}(p') (A_S \bar{G}_S - B_S \bar{G}_P \gamma_5) p(p). \end{aligned} \quad (33)$$

and

$$\begin{aligned} \langle n(p') | J^{(-)\mu\nu} | p(p) \rangle &= \langle n(p') | \bar{d} \sigma^{\mu\nu} (1 + \gamma_5) u | p(p) \rangle \\ &= i V_{ud} \bar{K}_{S,P} \bar{n}(p') (\Gamma^\mu \tilde{\Gamma}^\nu - \tilde{\Gamma}^\mu \Gamma^\nu) p(p) \\ &= \frac{i}{2M} V_{ud} \bar{n}(p') (\bar{K}_S \Pi_1^{\mu\nu} + \bar{K}_P \Pi_2^{\mu\nu} \gamma_5) p(p), \end{aligned} \quad (34)$$

The form factors become

$$\begin{aligned} \bar{G}_S(t) &= r_N F_1^V(t), \quad \text{with } r_N = \frac{M_n - M_p}{m_d - m_u} \sim \mathcal{O}(1), \\ \bar{G}_P(t) &= - \left(F_A(t) \left(\frac{M_n - M_p}{m_d - m_u} \right) - F_P(t) \frac{m_d + m_u}{M} \right), \end{aligned} \quad (35)$$

and

$$\begin{aligned} \bar{K}_S &= - \frac{M (M_n^2 - M_p^2) - (m_d^2 - m_u^2)}{4t (M_n - M_p)} \frac{\bar{G}_S}{F_A F_P}, \\ \bar{K}_P &= - \frac{M (M_n^2 - M_p^2) - (m_d^2 - m_u^2)}{4t (M_n + M_p)} \frac{\bar{G}_P}{F_1 F_P}. \end{aligned} \quad (36)$$

The effect of the scalar-tensor interactions at detection, on the asymmetry parameter A is shown in Fig. 5. We can make the following observation:

- With no NSI along propagation there can be difference for the A parameter between the two hierarchies though it is always positive. This difference in A is more appreciable for the LBNO baseline compared to the DUNE experiment.
- When NSI along propagation is included large differences in the A parameter is possible for both the baselines specially at larger energies. For both baselines the A parameter increases with energy for NH and decreases with energy for the IH. For the LBNO baseline, the crossing point when no NSI at detection is considered happens at $E_\nu = 5$ GeV and $A = 0$. When $S + T$ contribution is included, the crossing point remains at the same energy value but at non-zero value of A . This means that a non-zero value of A can be observed, but still the MH would not be resolved.

The effect of the $V \pm A$ interactions at detection, on the asymmetry parameter A is shown in Fig. 6. The $V \pm A$ interactions are more tightly constrained than the $S + T$ models and so in this case the effect of NSI at detection on the A parameter is modest and the general features of the A parameter does not alter significantly when compared with no NSI at detection.

In conclusion, in this work we explored resolving the MH using the $\nu_\mu \rightarrow \nu_\tau$ and $\bar{\nu}_\mu \rightarrow \bar{\nu}_\tau$ appearance channels. The determination of the mass hierarchy in these channels has an advantage over $\nu_\mu \rightarrow \nu_e$ as $P(\nu_\mu \rightarrow \nu_\tau)$ is not suppressed by small oscillation parameters as in the case for $P(\nu_\mu \rightarrow \nu_e)$. We also considered NSI effects along propagation and at detection for these channels. These transitions can be accessible with good precision for baseline as in the LBNO experiment. The DUNE experiment will have access to these channels but with less number of events. To resolve the MH, we introduced an asymmetry parameter defined as the difference of the two probabilities $P(\nu_\mu \rightarrow \nu_\tau)$ and $P(\bar{\nu}_\mu \rightarrow \bar{\nu}_\tau)$ normalized to their sum. The energy range of the LBNO and DUNE experiments is (0 – 10) GeV, where the quasielastic (QE) scattering is

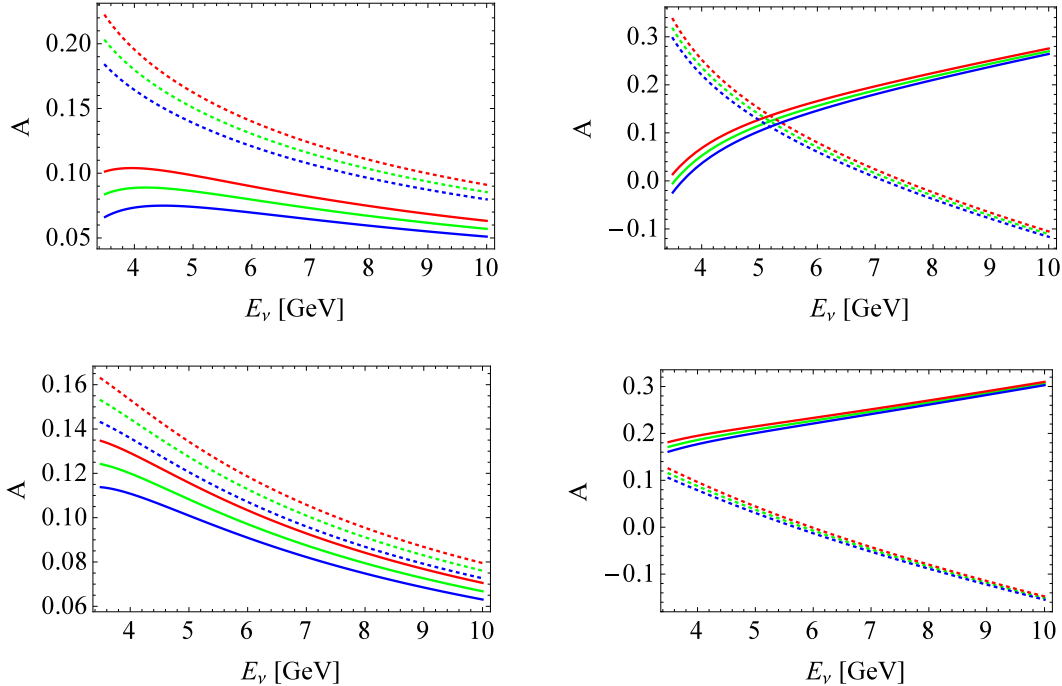


FIG. 5: $S + T$ model: The asymmetry parameter A for the energy range and baseline relevant to LBNO (top) and DUNE (bottom) experiments, where quasielastic effect is dominant. The solid/dotted lines correspond to NH/IH. The green, red, and blue lines correspond to $\delta = (0, \pi/2, -\pi/2)$, respectively, with $(S_R, S_L, T_L) = (-1.87, -1.31, 0.18)$. Left Panel: NSI parameters are taken to be $(\varepsilon_{\mu\tau}, \varepsilon_{\tau\tau}) = (0, 0)$. Right Panel: NSI parameters are taken to be $(\varepsilon_{\mu\tau}, \varepsilon_{\tau\tau}) = (0.07, 0.147)$.

dominant. We found that in this energy region the asymmetry parameter is positive for inverted hierarchy and negative for normal hierarchy when NSI are ignored. The prospect for resolving the hierarchy is much better for a LBNO type baseline. But when NSI along propagation is considered, the sign of A is flipped as we vary the energy. In both LBNO and DUNE baselines appreciable differences between the A parameters for the two hierarchies can arise. This gives a clear signal of the mass hierarchy as well as NSI. The pattern of the asymmetry parameter was found to be modestly sensitive to the CP phase. We considered NSI at detection in an effective Hamiltonian framework with generic vector axial-vector, scalar, and tensor interactions. The parameters in the effective Hamiltonian are constrained by τ decays. We found the $S + T$ model could have significant impact on the A parameter though the MH could still be resolved in a LBNO type baseline and in DUNE if NSI in propagation is present.

Acknowledgements: A.R acknowledges the hospitality of ICTP, Trieste, Italy during a visit when this work was in progress. This work was financially supported in part by the National Science Foundation under Grant No.NSF PHY-1414345.

-
- [1] F. P. An *et al.* [Daya-Bay Collaboration], *Phys. Rev. Lett.* **108** (2012) 17803 [arXiv:1203.1669]; F. P. An *et al.* [Daya-Bay Collaboration] [arXiv:1210.6327]. J.K. Ahn *et al.* [RENO Collaboration], [arXiv:1204.0626], *Phys. Rev. Lett.* **108** (2012) 191802; Y. Abe *et al.* [Double Chooz Collaboration] [arXiv:1207.6632]; T. Nakaya [for the T2K Collaboration], talk at Neutrino 2012; see also: K. Abe *et al.* [T2K Collaboration], *Phys. Rev. Lett.* **107** (2011) 041801 [arXiv:1106.2822].
- [2] J. Strait *et al.* [DUNE Collaboration], arXiv:1601.05823 [physics.ins-det].

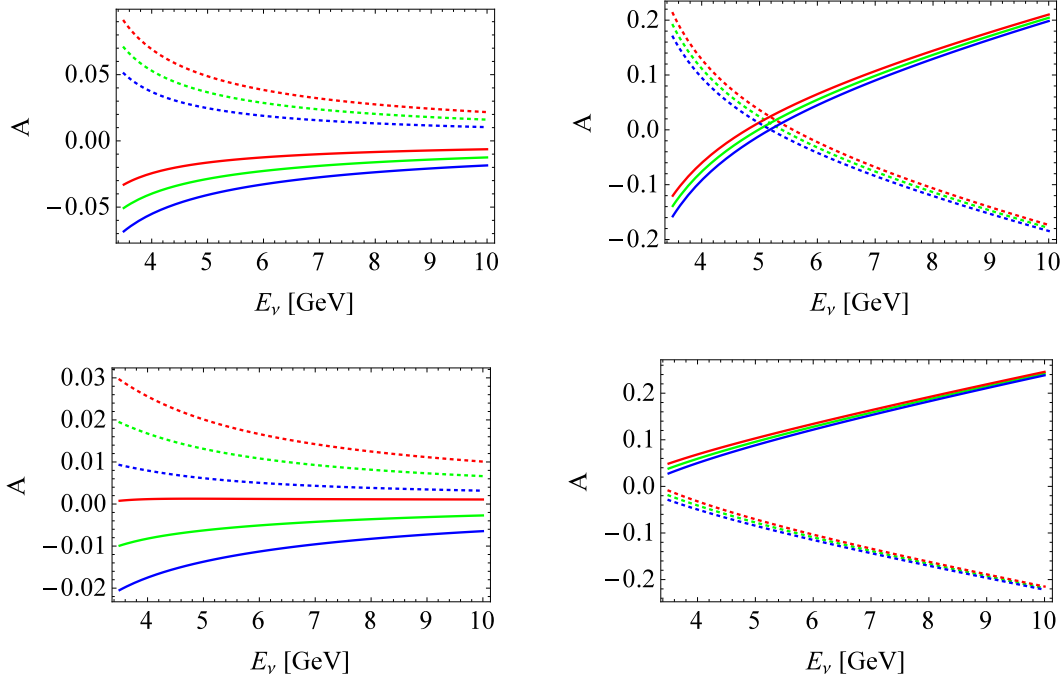


FIG. 6: $V\pm A$ model: The asymmetry parameter A for the energy range and baseline relevant to LBNO (top) and DUNE (bottom) experiments, where quasielastic effect is dominant. The solid/dotted lines correspond to NH/IH. The green, red, and blue lines correspond to $\delta = (0, \pi/2, -\pi/2)$, respectively, with $(V_L, V_R) = (0.016, 0.006)$. Left Panel: NSI parameters are taken to be $(\varepsilon_{\mu\tau}, \varepsilon_{\tau\tau}) = (0, 0)$. Right Panel: NSI parameters are taken to be $(\varepsilon_{\mu\tau}, \varepsilon_{\tau\tau}) = (0.07, 0.147)$.

- [3] R. Acciarri *et al.* [DUNE Collaboration], arXiv:1601.05471 [physics.ins-det].
- [4] R. Acciarri *et al.* [DUNE Collaboration], arXiv:1601.02984 [physics.ins-det].
- [5] R. Acciarri *et al.* [DUNE Collaboration], arXiv:1512.06148 [physics.ins-det].
- [6] K. Abe *et al.* [Hyper-Kamiokande Working Group Collaboration], arXiv:1412.4673 [physics.ins-det].
- [7] K. Abe, T. Abe, H. Aihara, Y. Fukuda, Y. Hayato, K. Huang, A. K. Ichikawa and M. Ikeda *et al.*, arXiv:1109.3262 [hep-ex].
- [8] S. K. Agarwalla *et al.* [LAGUNA-LBNO Collaboration], JHEP **1405**, 094 (2014) [arXiv:1312.6520 [hep-ph]].
- [9] S. K. Agarwalla *et al.* [LAGUNA-LBNO Collaboration], arXiv:1412.0593 [hep-ph].
- [10] M. S. Athar *et al.* [INO Collaboration], INO-2006-01.
- [11] E. K. Akhmedov, S. Razzaque and A. Y. Smirnov, JHEP **1302**, 082 (2013) [JHEP **1307**, 026 (2013)] [arXiv:1205.7071 [hep-ph]].
- [12] T. Ohlsson, H. Zhang and S. Zhou, Phys. Rev. D **88**, no. 1, 013001 (2013) doi:10.1103/PhysRevD.88.013001 [arXiv:1303.6130 [hep-ph]]. P. Coloma, A. Donini, J. Lopez-Pavon and H. Minakata, JHEP **1108**, 036 (2011) doi:10.1007/JHEP08(2011)036 [arXiv:1105.5936 [hep-ph]]. M. Masud, A. Chatterjee and P. Mehta, arXiv:1510.08261 [hep-ph]. J. S. Diaz, arXiv:1506.01936 [hep-ph].
- [13] J. P. Lees *et al.* [BaBar Collaboration], “Measurement of an Excess of $\bar{B} \rightarrow D^{(*)}\tau^-\bar{\nu}_\tau$ Decays and Implications for Charged Higgs Bosons,” Phys. Rev. D **88**, no. 7, 072012 (2013) doi:10.1103/PhysRevD.88.072012 [arXiv:1303.0571 [hep-ex]].
- [14] M. Huschle *et al.* [Belle Collaboration], Phys. Rev. D **92**, no. 7, 072014 (2015) doi:10.1103/PhysRevD.92.072014 [arXiv:1507.03233 [hep-ex]].
- [15] R. Aaij *et al.* [LHCb Collaboration], Phys. Rev. Lett. **115**, no. 11, 111803 (2015) Addendum: [Phys. Rev. Lett. **115**, no. 15, 159901 (2015)] doi:10.1103/PhysRevLett.115.159901, 10.1103/PhysRevLett.115.111803 [arXiv:1506.08614 [hep-ex]].
- [16] S. Fajfer, J. F. Kamenik and I. Nisandzic, [arXiv:1203.2654 [hep-ph]]; Y. Sakaki and H. Tanaka,

- [arXiv:1205.4908 [hep-ph]].
- [17] See for example: A. Datta, M. Duraishamy and D. Ghosh, “Diagnosing New Physics in $b \rightarrow c\tau\nu_\tau$ decays in the light of the recent BaBar result,” Phys. Rev. D **86**, 034027 (2012) doi:10.1103/PhysRevD.86.034027 [arXiv:1206.3760 [hep-ph]]; M. Freytsis, Z. Ligeti and J. T. Ruderman, “Flavor models for $\bar{B} \rightarrow D^{(*)}\tau\bar{\nu}$,” Phys. Rev. D **92**, no. 5, 054018 (2015) doi:10.1103/PhysRevD.92.054018 [arXiv:1506.08896 [hep-ph]].
- [18] A review of the R_{D^*} puzzle can be found in A. Greljo, G. Isidori and D. Marzocca, “On the breaking of Lepton Flavor Universality in B decays,” JHEP **1507**, 142 (2015) doi:10.1007/JHEP07(2015)142 [arXiv:1506.01705 [hep-ph]].
- [19] A. Filipuzzi, J. Portoles and M. Gonzalez-Alonso, Phys. Rev. D **85**, 116010 (2012) doi:10.1103/PhysRevD.85.116010 [arXiv:1203.2092 [hep-ph]]; B. Bhattacharya, A. Datta and D. London, arXiv:1603.03779 [hep-ph].
- [20] R. Aaij *et al.* [LHCb Collaboration], “Test of lepton universality using $B^+ \rightarrow K^+\ell^+\ell^-$ decays,” Phys. Rev. Lett. **113**, 151601 (2014) [arXiv:1406.6482 [hep-ex]].
- [21] G. Hiller and F. Kruger, “More model independent analysis of $b \rightarrow s$ processes,” Phys. Rev. D **69**, 074020 (2004) [arXiv:hep-ph/0310219]; C. Bobeth, G. Hiller and G. Piranishvili, “Angular distributions of anti-B $\rightarrow \ell^+ K$ anti- $\ell^+ \ell^-$ decays,” JHEP **0712**, 040 (2007) [arXiv:0709.4174 [hep-ph]]; C. Bouchard *et al.* [HPQCD Collaboration], “Standard Model Predictions for $B \rightarrow K\ell^+\ell^-$ with Form Factors from Lattice QCD,” Phys. Rev. Lett. **111**, no. 16, 162002 (2013) [Erratum-ibid. **112**, no. 14, 149902 (2014)] [arXiv:1306.0434 [hep-ph]].
- [22] See for example: S. L. Glashow, D. Guadagnoli and K. Lane, “Lepton Flavor Violation in B Decays?,” Phys. Rev. Lett. **114**, 091801 (2015) doi:10.1103/PhysRevLett.114.091801 [arXiv:1411.0565 [hep-ph]]. B. Bhattacharya, A. Datta, D. London and S. Shivashankara, “Simultaneous Explanation of the R_K and $R(D^{(*)})$ Puzzles,” Phys. Lett. B **742**, 370 (2015) doi:10.1016/j.physletb.2015.02.011 [arXiv:1412.7164 [hep-ph]].
- [23] P. Adamson *et al.* [MINOS Collaboration], Phys. Rev. D **88**, no. 7, 072011 (2013) doi:10.1103/PhysRevD.88.072011 [arXiv:1303.5314 [hep-ex]].
- [24] G. Mitsuka *et al.* [Super-Kamiokande Collaboration], Phys. Rev. D **84**, 113008 (2011) doi:10.1103/PhysRevD.84.113008 [arXiv:1109.1889 [hep-ex]].
- [25] S. Choubey, A. Ghosh, T. Ohlsson and D. Tiwari, JHEP **1512**, 126 (2015) doi:10.1007/JHEP12(2015)126 [arXiv:1507.02211 [hep-ph]].
- [26] A. Rashed, M. Duraishamy and A. Datta, Phys. Rev. D **87**, no. 1, 013002 (2013) [arXiv:1204.2023 [hep-ph]].
- [27] A. Rashed, P. Sharma and A. Datta, Nucl. Phys. B **877**, 662 (2013) [arXiv:1303.4332 [hep-ph]].
- [28] H. Liu, A. Rashed and A. Datta, arXiv:1505.04594 [hep-ph].
- [29] M. Masud and P. Mehta, arXiv:1603.01380 [hep-ph].
- [30] K. A. Olive *et al.* [Particle Data Group Collaboration], Chin. Phys. C **38**, 090001 (2014). doi:10.1088/1674-1137/38/9/090001
- [31] T. Teshima and T. Sakai, Analysis of atmospheric neutrino oscillations in three flavor neutrinos, Phys. Rev. D **62**, 113010 (2000) [hep-ph/0003038].
- [32] T. Kikuchi, H. Minakata and S. Uchinami, JHEP **0903**, 114 (2009) doi:10.1088/1126-6708/2009/03/114 [arXiv:0809.3312 [hep-ph]].
- [33] D. Meloni, T. Ohlsson and H. Zhang, JHEP **0904**, 033 (2009) doi:10.1088/1126-6708/2009/04/033 [arXiv:0901.1784 [hep-ph]].
- [34] T. Ohlsson, Rept. Prog. Phys. **76**, 044201 (2013) doi:10.1088/0034-4885/76/4/044201 [arXiv:1209.2710 [hep-ph]].
- [35] S. K. Agarwalla, Y. Kao, D. Saha and T. Takeuchi, JHEP **1511**, 035 (2015) doi:10.1007/JHEP11(2015)035 [arXiv:1506.08464 [hep-ph]].
- [36] A. M. Dziewonski and D. L. Anderson, *Preliminary reference earth model, Physics of the Earth and Planetary Interiors* **25** (1981) 297–356.
- [37] S. K. Agarwalla, T. Li, and A. Rubbia, *An Incremental approach to unravel the neutrino mass hierarchy and CP violation with a long-baseline Superbeam for large θ_{13}* , JHEP **1205** (2012) 154, [arXiv:1109.6526].
- [38] A. Stahl, C. Wiebusch, A. Guler, M. Kamiscioglu, R. Sever, et al., *Expression of Interest for a very long baseline neutrino oscillation experiment (LBNO)*, CERN-SPSC-2012-021, SPSC-EOI-007.
- [39] T. Bhattacharya, V. Cirigliano, S. D. Cohen, A. Filipuzzi, M. Gonzalez-Alonso, M. L. Graesser, R. Gupta and H. -W. Lin, Phys. Rev. D **85**, 054512 (2012) [arXiv:1110.6448 [hep-ph]]; C. -H. Chen and C. -Q. Geng, Phys. Rev. D **71**, 077501 (2005) [hep-ph/0503123].
- [40] K. Hagiwara, K. Mawatari and H. Yokoya, Nucl. Phys. B **668**, 364 (2003) [Erratum-ibid. B **701**, 405 (2004)] [hep-ph/0305324].

- [41] C. H. Llewellyn Smith, Phys. Rept. **3**, 261 (1972).
- [42] F. S. Queiroz, K. Sinha and A. Strumia, Phys. Rev. D **91**, no. 3, 035006 (2015) [arXiv:1409.6301 [hep-ph]].
- [43] W. Buchmuller, R. Ruckl and D. Wyler, Phys.Lett. B 191 (1987) 442.
- [44] I. Dorsner, S. Fajfer, N. Kosnik and I. Nisandzic, JHEP **1311**, 084 (2013) [arXiv:1306.6493 [hep-ph]].
- [45] K. G. Chetyrkin, Phys. Lett. B **404**, 161 (1997) [hep-ph/9703278].
- [46] J. A. Gracey, Phys. Lett. B **488**, 175 (2000) [hep-ph/0007171].